DAVID W. TAYLOR NAVAL SHIP RESEARCH AND DEVELOPMENT CENTER

Bethesda, Maryland 20084

DEVELOPMENT OF ADVANCED CIRCULATION CONTROL WING HIGH LIFT AIRFOILS

by

Robert J. Englar
Gregory G. Huson

APPROVED FOR PUBLIC RELEASE: DISTRIBUTION UNLIMITED

Reprint of AIAA Paper 83-1847
Presented at the AIAA Applied Aerodynamics Conference
Danvers, Massachusetts
13-15 July 1983

AVIATION AND SURFACE EFFECTS DEPARTMENT
RESEARCH AND DEVELOPMENT REPORT

December 1983

DTNSRDC-83/109

MAJOR DTNSRDC ORGANIZATIONAL COMPONENTS

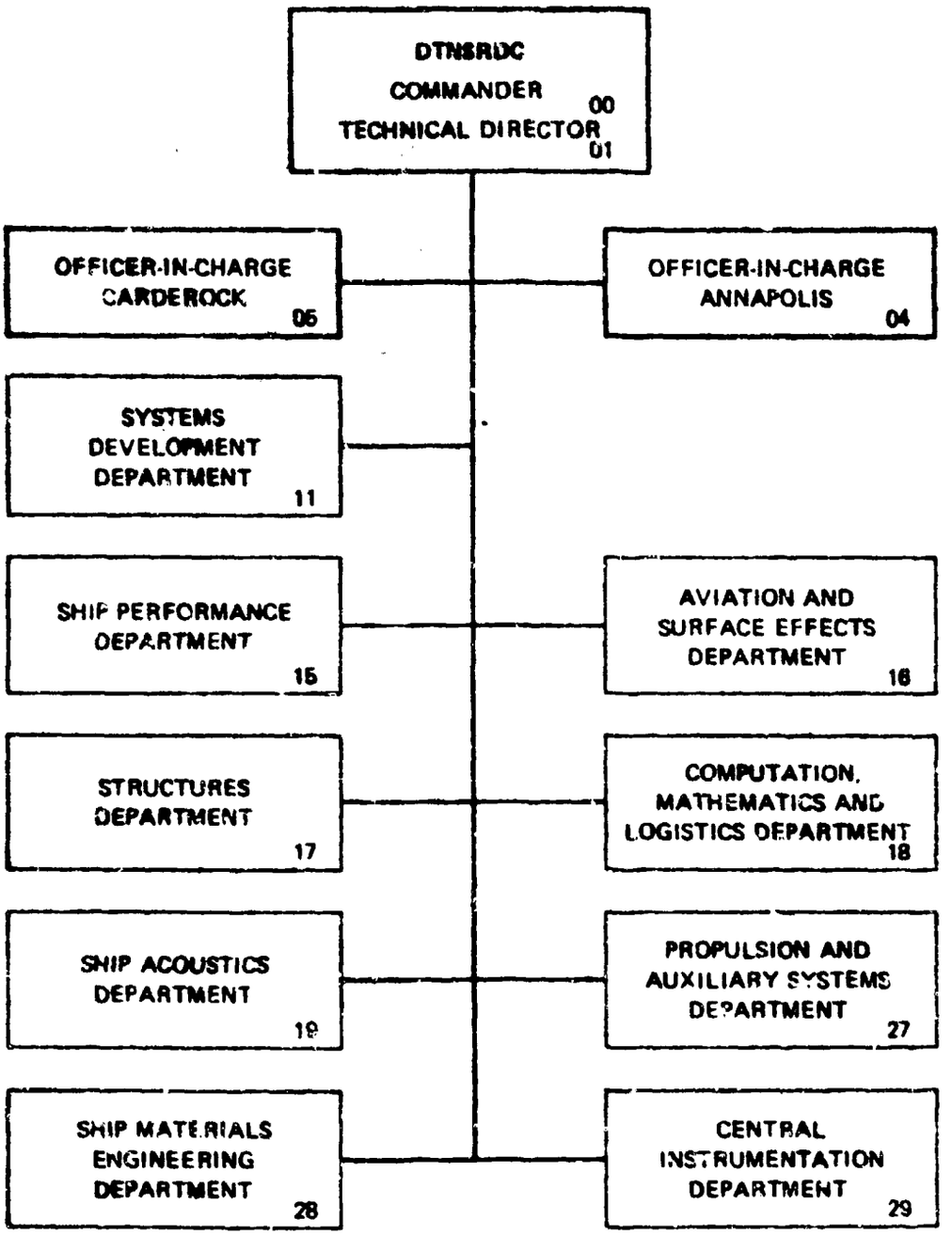

UNCLASSIFIED

SECURITY CLASSIFICATION OF THIS PAGE (When Data Entered)

REPORT DOCUMENTATION PAGE		READ INSTRUCTIONS BEFORE COMPLETING FORM
1. REPORT NUMBER DTNSRDC-83/109	2. GOVT ACCESSION NO. AD-A136585	3. RECIPIENT'S CATALOG NUMBER
4. TITLE (and Subtitle) DEVELOPMENT OF ADVANCED CIRCULATION CONTROL WING HIGH LIFT AIRFOILS		5. TYPE OF REPORT & PERIOD COVERED Interim report Oct 82 - July 83
		6. PERFORMING ORG. REPORT NUMBER Aero Report 1289
7. AUTHOR(s) Robert J. Englar Gregory G. Huson		8. CONTRACT OR GRANT NUMBER(s)
9. PERFORMING ORGANIZATION NAME AND ADDRESS David W. Taylor Naval Ship Research and Development Center Bethesda, Maryland 20084		10. PROGRAM ELEMENT, PROJECT, TASK AREA & WORK UNIT NUMBERS Program Element 62241N Task Area WF 41.421 Work Unit 1600-831
11. CONTROLLING OFFICE NAME AND ADDRESS Naval Air Systems Command (AIR 310D) Washington, D.C. 20361		12. REPORT DATE December 1983
		13. NUMBER OF PAGES 18
14. MONITORING AGENCY NAME & ADDRESS(if different from Controlling Office)		15. SECURITY CLASS. (of this report) UNCLASSIFIED
		15a. DECLASSIFICATION/DOWNGRADING SCHEDULE

16. DISTRIBUTION STATEMENT (of this Report)

APPROVED FOR PUBLIC RELEASE: DISTRIBUTION UNLIMITED

17. DISTRIBUTION STATEMENT (of the abstract entered in Block 20, if different from Report)

18. SUPPLEMENTARY NOTES

Reprint of AIAA Paper 83-1847. Presented at the AIAA Applied Aerodynamics Conference, Danvers, Massachusetts, 13-15 July 1983.

19. KEY WORDS (Continue on reverse side if necessary and identify by block number)

Circulation Control Wing
High Lift Aerodynamics
Two-Dimensional Airfoils
STOL
Supercritical Airfoil

20. ABSTRACT (Continue on reverse side if necessary and identify by block number)

Recent experimental and flight test programs have developed and confirmed the high lift capability of the Circulation Control Wing (CCW) concept. These CCW airfoils employ tangential blowing of engine bleed air over circular or near circular trailing edges, and are capable of usable lift coefficients triple those of simple mechanical flaps. Earlier versions of these blown airfoils made use of relatively complex leading and trailing edge devices which-

(Continued on reverse side)

DD FORM 1 JAN 73 1473 EDITION OF 1 NOV 65 IS OBSOLETE
S/N 0102-LF-014-6601

UNCLASSIFIED

SECURITY CLASSIFICATION OF THIS PAGE (When Data Entered)

(Block 20 continued)

would have to be retracted mechanically for cruise flight. In a continuing program to reduce the complexity, size and weight of the CCW system, several series of advanced CCW airfoils have been developed which can provide STOL capability for both military and commercial aircraft using much smaller, less complex high lift systems. This paper describes these configurations and presents the experimental results confirming their aerodynamic characteristics, ~~as well as make~~ comparisons to previous CCW and more conventional high lift systems.

→ are provided.

Accession For	
NTIS GRA&I	☒
DTIC TAB	☐
Unannounced	☐
Justification	
By	
Distribution/	
Availability Codes	
Dist	Avail and/or Special
A-1	

TABLE OF CONTENTS

LIFT OF FIGURES

AIAA'83

AIAA-83-1847

Development of Advanced Circulation Control Wing High Lift Airfoils

R.J. Englar and G.G. Huson,
David Taylor Naval Ship Research and Development Center, Bethesda, MD

AIAA
Applied Aerodynamics Conference

July 13-15, 1983
Danvers, Massachusetts

DEVELOPMENT OF ADVANCED CIRCULATION CONTROL WING HIGH LIFT AIRFOILS

Robert J. Englar* and Gregory G. Huson +

STOL Aerodynamics Group, Aircraft Division
David Taylor Naval Ship Research and Development Center
Bethesda, Maryland 20084

Abstract

Recent experimental and flight test programs have developed and confirmed the high lift capability of the Circulation Control Wing (CCW) concept. These CCW airfoils employ tangential blowing of engine bleed air over circular or near-circular trailing edges, and are capable of usable lift coefficients triple those of simple mechanical flaps. Earlier versions of these blown airfoils made use of relatively complex leading and trailing edge devices which would have to be retracted mechanically for cruise flight. In a continuing program to reduce the complexity, size and weight of the CCW system, several series of advanced CCW airfoils have been developed which can provide STOL capability for both military and commercial aircraft using much smaller, less complex high lift systems. The paper will describe these configurations and present the experimental results confirming their aerodynamic characteristics, as well as make comparisons to previous CCW and more conventional high lift systems.

Introduction

The development of high lift airfoils employing tangential blowing over round or near-round trailing edges has been underway at David Taylor Naval Ship R&D Center since 1969.[1] Recent experimental and flight test programs[2-5] have confirmed the high lift and STOL capabilities of this Circulation Control Wing (CCW) concept. As applied to a typical fixed-wing aircraft, the concept employs engine bleed air to pneumatically augment the wing's circulation lift, and has generated section lift coefficients as much as triple those of simple mechanical flaps. The application of this lift to provide STOL capability was flight-verified in 1979, when a rather large radius (0.0365 chord) CCW trailing edge was applied to the wing of a NAVY/Grumman A-6 testbed aircraft. Figure 1 shows the wing-fold airfoil section evaluated two-dimensionally prior to the flight demonstrator development. Figure 2 records the increased lifting capability provided by the trailing edge blowing. The effectiveness of this round CCW trailing edge in augmenting wing lift resulted in significant STOL performance and heavy lift potential[4,6]. A demonstrated 140 percent increase in usable trimmed lift coefficient produced reductions of 35 percent in approach speed, 60 percent in takeoff distance and 65 percent in landing ground roll relative to the standard A-6. Flight speeds as low as 67 kt were achieved by the A-6/CCW aircraft.

These flight results confirmed CCW as a simple and effective blown STOL system, but also identified several improvements needed before the system could be incorporated into production aircraft. The large trailing edge radius demonstrated on the A-6/CCW aircraft ensured high lift augmentation but was not acceptable from a cruise drag standpoint. It would either have to be mechanically retracted, or its size reduced to the point where the base thickness was no longer a penalty. A second problem area was the leading edge device required to prevent flow separation during the high circulation associated with STOL operation. Whereas the 37.5-degree slat deflection on the 2-D model had proved sufficient, the flight demonstrator maximum deflection was mechanically limited to 25 degrees. Therefore, an increased leading edge radius had been added to the testbed aircraft and it performed quite satisfactorily. However, for cruise flight, it too would have to be retracted. A feasible alternative would be to revise the mechanical actuator/track system to allow greater deflection.

In order to address these areas of needed improvement, a program has been underway since the flight test to develop advanced CCW airfoils by reducing the complexity, size and weight of the CCW system without penalizing its lift aug-

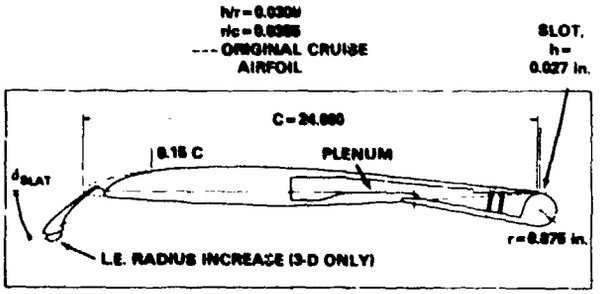

Fig. 1 - A-6/CCW Wing-Fold Airfoil Section (64A008.4/CCW), $\delta_{SLAT} = 37.5°$, Large Trailing Edge Radius

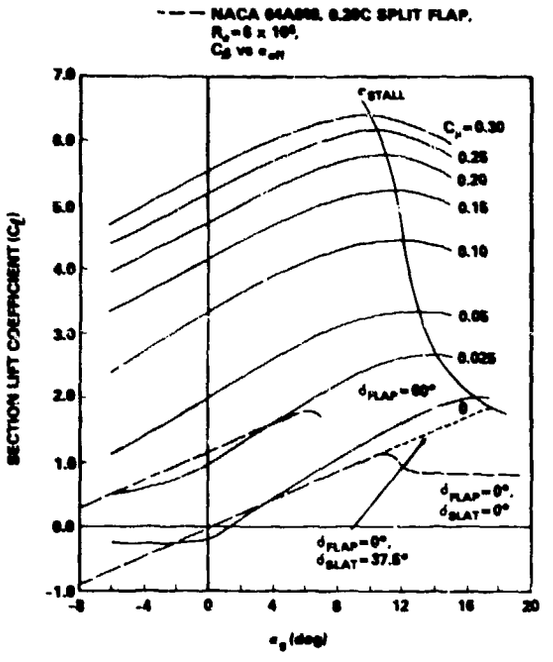

Fig. 2 - Lift Characteristics of the NACA 64A008.4/CCW Airfoil, $\delta_{SLAT} = 37.5°$, $r/c' = 0.0365$

*CCW Program Manager; Associate Fellow, AIAA
+ Aerospace Engineer; Member, AIAA

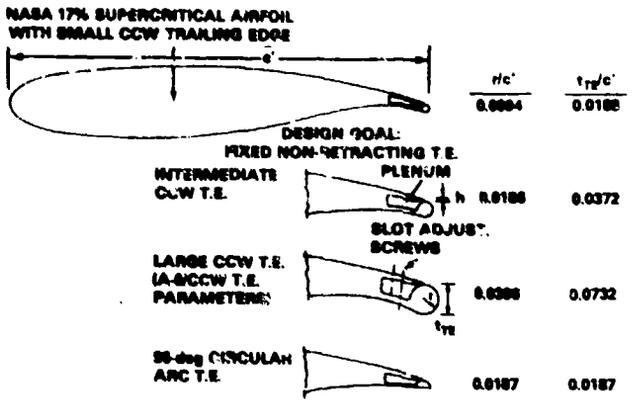

Fig. 3 - CCW/Supercritical Airfoil Model Geometries

menting capability. That program has proceeded in two directions: (1) to develop an advanced CCW airfoil which would incorporate a smaller trailing edge, blown plenum and a non-deflecting leading edge device all within the contour of an existing supercritical airfoil which could replace current state-of-the-art wing sections, and (2) to develop improved versions of CCW which are compatable with existing thin wings such as those already on the A-6 and other current high performance aircraft. In both cases, maintaining lift augmentation while reducing drag and complexity have been the dominant goals of the program. The following sections will discuss the design considerations and experimental evaluations involved in the development of these airfoils, and compare the performance to the earlier relatively complex CCW configurations.

Design Considerations

CCW/Supercritical Airfoil

The above goals appeared to be obtainable by taking advantage of the large leading and trailing edge thickness of a typical bluff trailing edge supercritical airfoil. Not only does this airfoil section geometry appear quite compatible with the incorporation of aft plenum, slot and small radius trailing edge, it also generates the excellent transonic cruise performance afforded by increased critical Mach number and delayed drag rise. The developmental approach taken was to combine a typical proven supercritical section with a set of baseline CCW trailing edge parameters closely matching those of the A-6/CCW aircraft, and then experimentally evaluate the characteristics produced by progressively reducing the trailing edge size until it was most compatible with the supercritical airfoil aft contour. The NASA 17-percent-thick supercritical airfoil of Reference 7 had been both wind-tunnel tested and flight tested, and therefore had a suitable reference data base. The airfoil thickness produces a large bluff leading edge radius of 4.2%-percent chord, which is of such substantial size that it could substitute for a mechanical leading edge device and thus further simplify the high-lift configuration. To parametrically vary the model trailing edge geometry, the A-6/CCW design radius-to-chord ratio of 0.0365 was taken as a baseline reference value, halved to give $r/c' = 0.0186$ and halved again to give $r/c' = 0.0094$. The smallest trailing edge diameter ($0.0188c'$) is thus slightly greater than twice the $0.008c$ trailing edge thickness of the baseline supercritical airfoil. These model configurations are shown in Figure 3, where the pertinent CCW trailing edge parameters are also identified. The terms r, h, c and c' represent trailing edge radius, jet slot height, original baseline airfoil chordlength, and effective airfoil chordlength including the radius, respectively.

Detailed discussion of the characteristics of these four airfoils is given in References 8 and 9; therefore, only the smallest radius configuration will be included in the following discussion of results.

A-6/CCW Airfoils

Because high performance aircraft typically employ thinner sections with sharp trailing edges, a second program was undertaken to extend the above smaller trailing edge CCW/Supercritical configurations to these thin airfoils. Because of the data base already established for the A-6 airfoil section, it was selected as the reference thin airfoil. The 8.4-percent airfoil of Figure 1 was modified to accept the CCW trailing edges shown in Figures 4 and 5. The "small" radius ($r/c' = 0.009$) is the same trailing edge configuration used with the supercritical airfoil, while the "mini" radius is half that size, yielding a cruise trailing edge diameter of $0.009c'$. Neither of these configurations is intended to be retracted in cruise, being 1/4 and 1/3 the size of the original flight-test trailing edge. The retractable circular arc configuration uses a simple rotating segment to produce 150 degrees of jet turning arc (as measured from the slot) when deflected for high lift, retracting to 96 degrees and a trailing edge thickness of $0.0178c'$ in cruise. It thus has a cruise base thickness slightly less than the small round configuration, but a radius roughly twice as large for effective jet turning. The dual radius configuration is in effect a very short chord ($0.0223c'$) blown flap, with several important differences. It pivots about a lower surface hinge point, with a radius the same as the small single-radius configuration ($0.009c'$), and deflects to 90 degrees. The aft surface is not straight like the conventional blow flap, but is a second much larger radius, $0.041c'$.

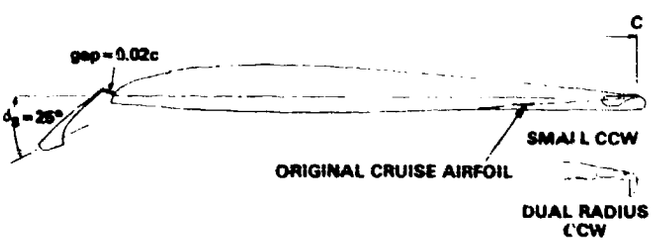

Fig. 4 - Incorporation of the Small CCW Geometries on the A-6/64A008.4 Airfoil

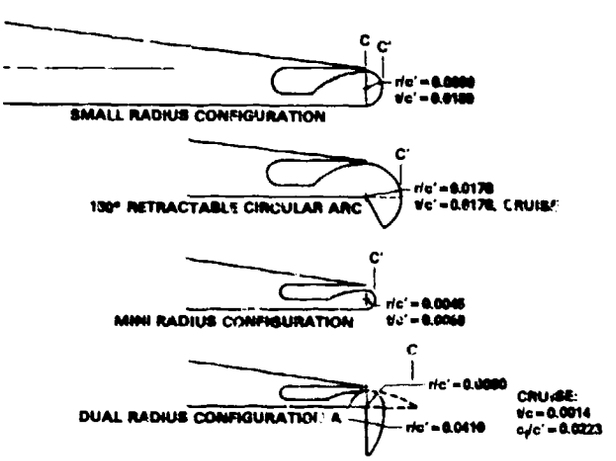

Fig. 5 - A-6/CCW Small Trailing Edge Detail and Parameters

This produces a downstream CC radius larger than the original flight demonstrator, but a cruise trailing edge thickness exactly the same as the clean A-6 airfoil, 0.0014c. The second radius adds additional jet deflection, so that when the flap is deflected 90 degrees, the maximum jet angle is 122 degrees from the slot. Jet attachment at this deflection should be enhanced by the larger radius. Two additional blown configurations were constructed and tested, and are shown in Figure 6. The 0.226c blown flap is a Grumman Aerospace Corporation design (see Reference 10) employing a straight aft upper surface and a radius downstream of the slot when the flap is deflected. A second dual radius CCW trailing edge, configuration B, has a larger flap chord than the first, intended to produce more lift due to geometric camber when the blowing is off. Its radii are increased (because the hinge point moves forward) to 0.012c' and 0.060c', but the cruise trailing edge thickness remains 0.0014c. Two additional deflection angles have been added: 0 degrees (cruise) and 60 degrees (intermediate lift at reduced drag, intended as a takeoff configuration). The maximum jet turning angles for the 0, 60, and 90 degree flap deflections are thus 33, 93, and 123 degrees, respectively, from the jet exit plane parallel to the chord.

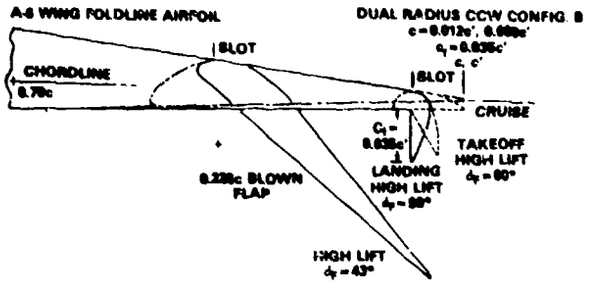

Fig. 6 - Dual Radius CCW and Blown Flap Configurations

Mention should be made of the design blowing momentum coefficients, C_μ (to be defined in the following section). Expected full scale values are functions of bleed mass flow and pressure available and the flight velocity (a function of weight, incidence, lift coefficient obtained with blowing, and engine vertical thrust component). For the A-6/CCW flight demonstrator using existing bleed from its J-52-P8B turbojet engines, available C_μ ranged up to 0.30. However, since current high performance aircraft may employ turbofan engines with less bleed capability, a limit on available momentum for these engines was estimated to yield $0.05 < C_\mu < 0.15$. Thus for the majority of the thin airfoil small trailing edge data, C_μ will be limited to approximately 0.17.

Experimental Apparatus and Technique

The 3-ft span two-dimensional models described above were mounted between the 3- by 8-ft subsonic two-dimensional wall inserts installed in the DTNSRDC 8- by 10-ft subsonic tunnel (Figure 7). Lift and moment coefficients were obtained by numerical integration of surface static pressures near the midspan as recorded by a 144-port scanivalve system. The drag coefficient was obtained from integration of wake momentum deficit as measured on a fixed wake rake spanning nearly 8-ft from floor to ceiling. All reported force and moment coefficients are based on c', since this is considered to be the undeflected cruise reference chord. The value c' may differ from c, the original baseline airfoil chord, in that the slot is located at the original trailing edge, and thus the new small CCW devices extend somewhat aft. The momentum coefficient C_μ was calculated as $\dot{m}V_j/(qc')$, where

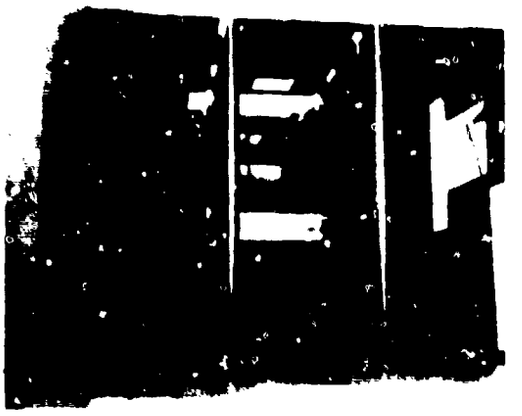

Fig. 7 - Airfoil Installed in the DTNSRDC 3- x 8-foot Subsonic 2-D Inserts

$\dot{m}$ is the mass flow per unit slot span as measured by venturimeter, and V_j is the isentropic jet velocity calculated from measured conditions using the equation in Reference 5. Model installation, test apparatus and technique, data reduction and corrections, and monitoring of tunnel two-dimensionality were all conducted as reported in Reference 5 (Appendix A) and Reference 11.

Results and Discussion

CCW/Supercritical Airfoil

The small radius configuration of Figure 3 was evaluated over a geometric angle of attack range $-5 \text{ degrees} \leq \alpha_g \leq +15$ degrees. The relatively low freestream dynamic pressure of 10 psf ($R_c = 1.2 \times 10^6$) yielded C_μ values up to 0.40 instead of the 0.17 limit mentioned above. Lift data for a slot height of 0.014 in. are presented in Figure 8 as functions of incidence and blowing. If these plots are compared to the state-of-the-art A-6/CCW airfoil data of Figure 2, which was run

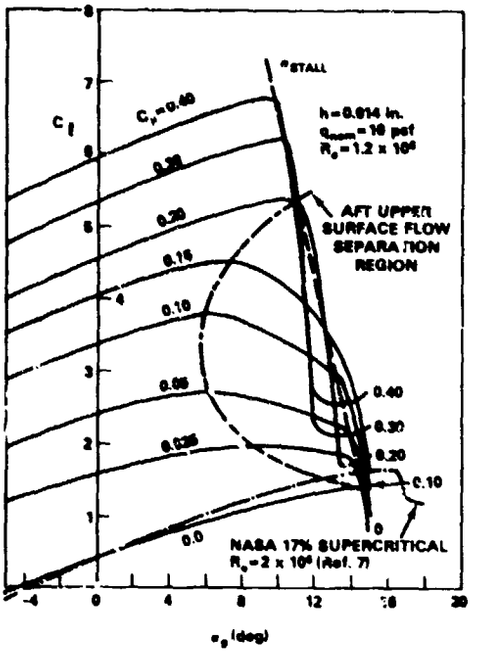

Fig. 8 - Variation in Lift with Incidence at Constant Blowing for the Small Trailing Edge CCW/Supercritical Airfoil

at a larger slot height and Reynolds number, two trends are noticeable. First, the CCW/Supercritical airfoil, with a radius only 25 percent as large, produces lift that is slightly greater than the A-6/CCW airfoil at lower α and C_μ, since the A-6 slat imparts a download under these conditions. Second, the undeflected bulbous nose of the supercritical airfoil provides the same or better leading edge performance as the A-6 model's 37.5-degree slat, yielding almost identical stall angles at any given C_ℓ.

The apparent deficits in certain of the lift curves (primarily for 6 degrees $\leq \alpha_g \leq$ 12 degrees and $C_\mu < 0.20$) are due to flow separation on the supercritical airfoil cambered aft upper surface, between the crest and the slot. (This condition is discussed in Reference 12 and is not a leading edge separation.) The separated flow is re-entrained at higher C_μ, and the deficits disappear. The same correction should occur at higher Reynolds numbers.

Drag polars for the small radius airfoil at low blowing values are compared in Figure 9 with the baseline 17-percent supercritical airfoil. The drag values of the baseline airfoil are slightly lower than those of the CCW/supercritical airfoil with no blowing ($\Delta C_d = 0.0006$ at $\alpha_g = 0$ degrees); however, the drag of the CCW airfoil can be reduced to that of the baseline airfoil by blowing at $C_\mu \leq 0.003$ for $\alpha_g \leq$ 6 degrees, typical values for cruise incidence. Additional blowing will reduce the drag even further, but an analysis of engine thrust loss due to bleed required needs to be considered.

For $R_c = 2 \times 10^6$ and $\alpha_g = 0$ degrees, unblown drag values for the small radius and a larger radius CCW/Supercritical airfoil are compared with both the baseline supercritical and a typical sharp trailing edge airfoil in the following chart:

Airfoil	C_d	C_ℓ
64_3-418 ($R_c = 3 \times 10^6$)	0.0061	0.330
Baseline supercritical	0.0084	0.400
Small CCW, r/c' = 0.0094	0.0090	0.455
Large CCW, r/c' = 0.0366	0.0183	0.671

As lift due to camber increases, so does the drag. At equal cruise lift, the drag of the baseline and small CCW airfoil will be nearly equal. Thus, the high-lift device of the small CCW/Supercritical airfoil may be left exposed for cruise conditions with essentially no subsonic drag penalty

A-6/CCW and Blown Airfoils

Lift Generation

The various CCW and blown flap configurations of Figures 4, 5, and 6 were evaluated extensively over a range of subsonic dynamic pressure, angle of attack, and jet slot height. The data comparisons that follow are intended primarily to show the effect of the configuration geometry changes on lift augmentation in the moderate blowing range of $C_\mu < 0.17$. It should be noted that while the original large radius A-6/CCW was tested with a 37.5-degree slat deflection to keep flow attached at high circulation levels associated with C_μ up to 0.30, the majority of the current tests were conducted with a slat deflection of 25 degrees and 0.02c gap. This is the slat setting on the production A-6, and was originally thought to be more appropriate for the lower blowing levels. This choice did not prove appropriate in certain cases, as will be discussed later.

Lift resulting from blowing at constant geometric angle of attack is shown in Figures 10-13 for the single-radius CCW

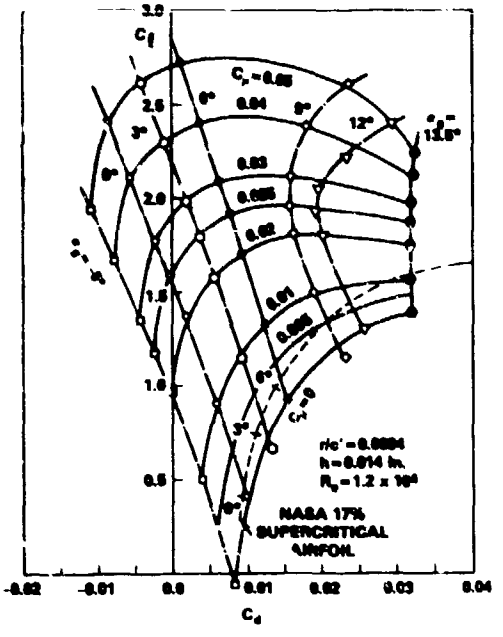

Fig. 9 - Drag Polars for the Small Trailing Edge CCW/Supercritical Airfoil at Low Blowing

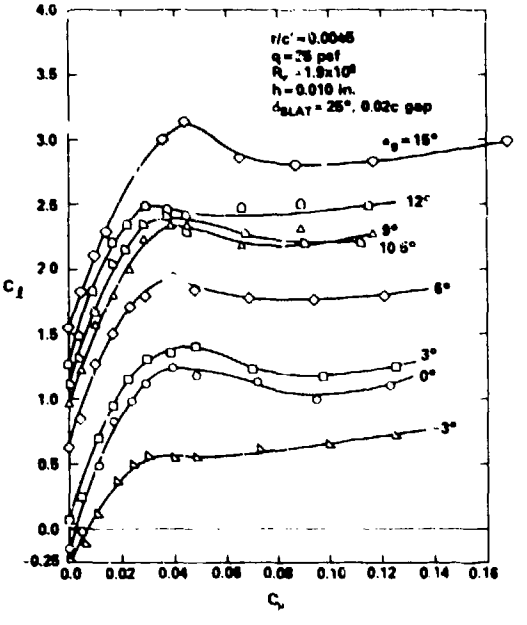

Fig. 10 - Lift Due to Blowing for the Mini Radius A-6/CCW Airfoil

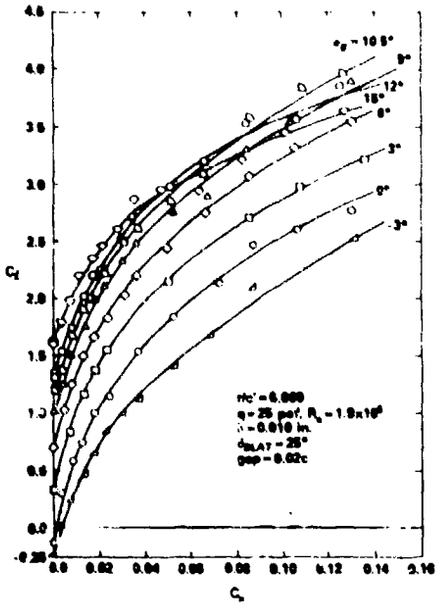

Fig. 11 - Lift Due to Blowing for the Small Radius A-6/CCW Airfoil

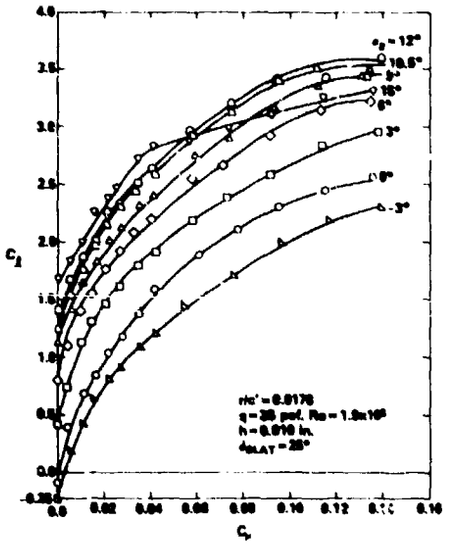

Fig. 12 - Lift Due to Blowing for the 96° Circular Arc A-6/CCW Airfoil

configurations. Greatest lift prior to stall is generated by the 150-degree circular arc, which has the largest radius. Apparently 150 degrees of jet turning surface is sufficient to keep the jet attached for this range of blowing and lift. However, the reduced lift produced by the same radius with only 96 degrees of turning implies that more turning arc is required. For the three round CCW trailing edges with adequate turning arc, lift generation is reduced as radius decreases. For the smallest radius (Figure 10) lift maxima occur at about $C_\mu = 0.04$, and augmentation beyond that is reduced. This same trend was noted in References 8 and 9 for the small radius supercritical airfoil, once certain pressure ratios were exceeded. In Figure 10, that pressure ratio for the mini radius is about 1.4 to 1.5, but was considerably higher for the CCW/Supercritical section twice the radius. Note also

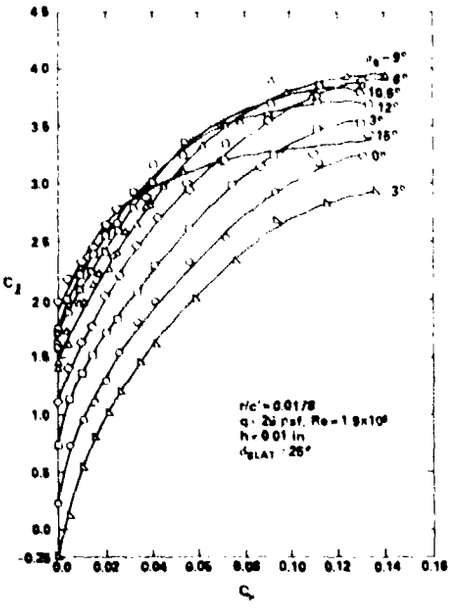

Fig. 13 - Lift Due to Blowing for the 150° Circular Arc A-6/CCW Airfoil

in Figures 11-13 that as the lift coefficient approaches 4 at constant C , stall occurs at the higher incidences, indicating that the 25-degree slat is unable to prevent leading edge separation at these circulation levels.

The favorable effect of increased trailing edge radius is further emphasized in Figures 14 and 15 for the two dual radius configurations. In Figure 14, the radius immediately downstream of the blowing slot is the same as in Figure 11, but the enlarged second radius is very effective in turning the

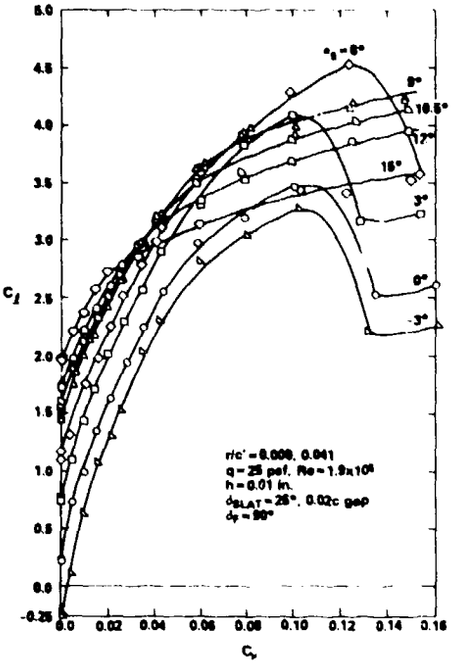

Fig. 14 - Lift Due to Blowing for Dual Radius CCW Configuration A, $c_f = 0.0223c'$

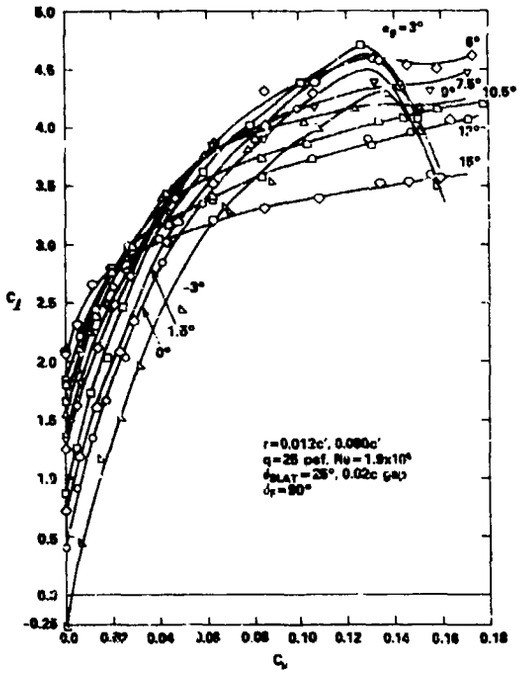

Fig. 15 - Lift Due to Blowing for Dual Radius Configuration B, $c_f = 0.035c'$

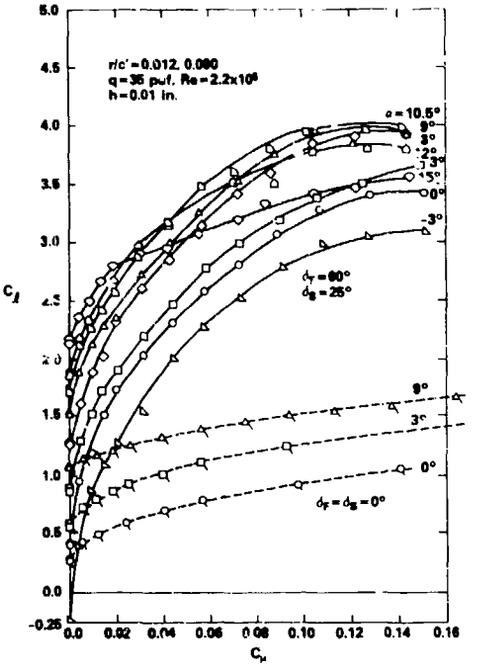

Fig. 16 - Lift Due to Blowing for Dual Radius Configuration B, $c_f = 0.035c'$, $\delta_F = 0°$, 60°

and enhancing lift. In addition, the camber provided by the 90-degree flap deflection adds 0.4 to 0.5 to lift coefficient, blowing off. Both these effects are further improved upon by dual radius configuration B, where increasing the flap chord moves the hinge point forward on the airfoil and allows the trailing edge radii to be increased to 0.012c' and 0.060c'. The second radius is 64 percent larger than the original airfoil of Figure 1, and results in increased jet turning. In addition to the increase in lift, configuration B pushes the lift peaks which occurred at $C_\mu = 0.10$ (pressure ratio of 2.0) in Figure 14 up to $C_\mu = 0.13$ (pressure ratio of 2.2). At angles of attack greater than 3 degrees, the peaks are minimal or nonexistant. Reference 8 data for the CCW/Supercritical airfoil indicate that these peaks may be moved to higher C_μ by reducing the jet slot height or further increasing the radius. Both airfoils again experience leading edge stall at high lift and incidence due to insufficient slat deflection.

Reduction in flap deflection reduces the airfoil geometric camber as well as the maximum angle through which the jet may turn. Those effects are shown in Figure 16 for 0- and 60-degree flap deflections. The zero-degree case becomes essentially a 33-degree jet flap, while the 60-degree flap produces 93 degrees of jet turning and appreciable lift. The advantages of these two configurations are lower drag due to reduced projected area and increased jet thrust recovery. The 60-degree flap could thus be effectively employed as a takeoff setting.

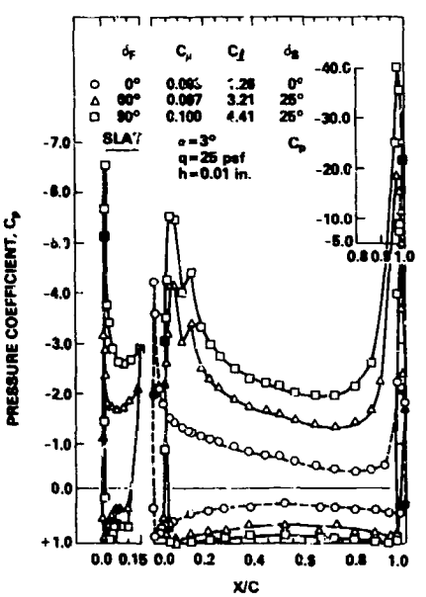

Fig. 17 - Pressure Distributions for Dual Radius Configuration B, $c_f = 0.035c'$

The pressure distributions in Figure 17 give further insight into the above discussion. The increased suction peaks produced over the trailing edge radii indicate why the lift is more than tripled by increasing the flap deflection from 0 to 90 degrees at $C_\mu = 0.10$. The $C_p = -40$ value shows why the larger radii are more effective: they are more able to prevent the high velocity jet from separating from the radius before sufficient turning is produced. The increased suction spike on the slat leading edge points to the nearness of leading edge stall at this slat deflection. Note in this figure that the slat pressures are plotted normal to the chord rather than deflected, and that the slat is retracted for the 0-degree flap case, since it represents a cruise configuration. The small spike at $x/c = 0.15$ is due to the exposed cove on the main airfoil which the slat trailing edge retracts into in cruise. The solid symbols are the leading and trailing edges of each separate element.

A-6 High Lift Airfoil Comparison

A summary comparison of all the above A-6 high lift configurations is presented in Figure 18 for a typical geometric incidence of 9 degrees. The large radius CCW airfoil data from Figure 2 have been adjusted to 25-degree slat deflection as a basis for comparison. Only the two dual radii configurations are superior to the original large configuration in lift, and they fall below the large surface at higher C_μ because the jet reaches the maximum turning angle (≈123 degrees). For the full-round large CCW, jet turning can continue on to 150 degrees or more. However, from a mechanization and drag standpoint, this large CCW is impractical, and thus most of the configurations shown offer significant operational improvement. To serve as a reference to the actual airplane, the single-slotted semi-Fowler flap ($c_f = 0.30c$) employed on the A-6 was also tested in connection with the Grumman test of Reference 10. For C_μ in the range of 0.05 or greater, all CCW airfoils tested exceed the mechanical flap's capability except for the mini radius configuration. Figure 19 shows a similar comparison for $\alpha_g = 3$ degrees, and includes the 0.226c blown flap configuration[10]. The leading edge stall problem is now avoided at the lower incidence, and the dual radius exceeds its Figure 18 performance at higher blowing. Both the 60-degree dual radius and the 0.226c blown flap behave in the typical blown flap manner: once flow is turned to the flap upper surface angle, the lift variation becomes nearly linear with C_μ, instead of the parabolic function typical of a round CCW. For $C_\mu > 0.026$, the 90-degree flap dual radius exceeds the 0.226c blown flap lift, even though it is less than 1/6 the chord length. The blown flap is superior at low and no blowing due to the extra camber produced by its longer chord length. All three of the CCW configurations can double the lift of the baseline single-slotted flap in the $C_\mu < 0.16$ range; the 0.226c blown flap can not.

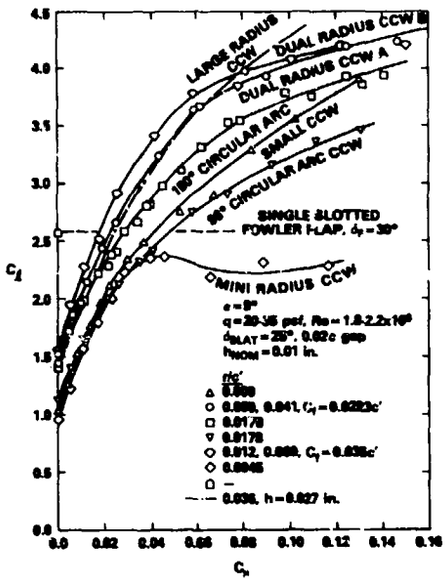

Fig. 18 - Comparative Blown Lift Configurations

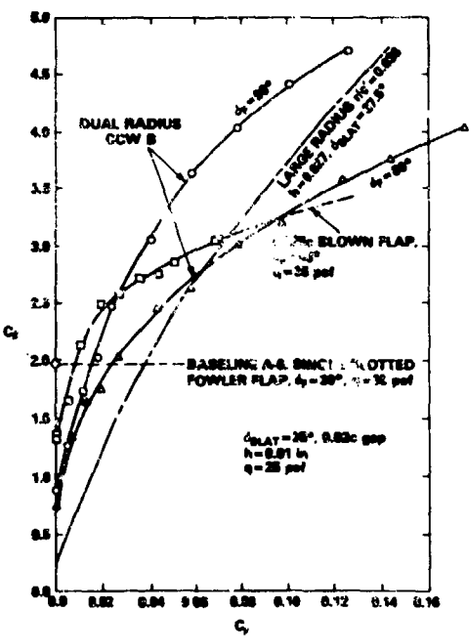

Fig. 19 - Comparative Lift Capability, $\alpha_g = 3°$

Lift variation with angle of attack is shown in Figure 20 for the larger-flap dual radius CCW. The effect of leading edge stall is apparent at higher C_μ. The variation in α_{stall} with lift for the 37.5-degree slat deflection (from Figure 2) is also plotted, and the present data are extrapolated to that line to show the effect of keeping the flow attached. At $C_\mu = 0.125$, stall progresses from $\alpha_g = 3.7$ degrees and $C_\ell = 4.7$ with the 25-degree slat to $\alpha_g = 11.5$ degrees and $C_\ell = 5.2$ with the 37.5-degree slat. For comparison, the clean A-6 airfoil and single-slotted flap A-6 airfoil data are shown: they were recorded in conjunction with the Grumman tests of Reference 10, but at q = 35 psf and $R_c = 2.2 \times 10^6$, which may explain why the stall angle somewhat exceeds the existing 25-degree slat curve. At a usable 2-D incidence of 9 degrees, the dual radius airfoil with 37.5-degree slat and $C_\mu = 0.125$ will yield $C_\ell = 5.2$ compared to 2.6 for the baseline mechanical flap. Comparing the dual radius data of Figure 20 (extrapolated for the flow-attaching 37.5-degree slat) to the original large chord A-6/CCW airfoil of Figure 2 shows significant improvement in lift over the whole range of blowing at least up to $C_\mu = 0.125$.

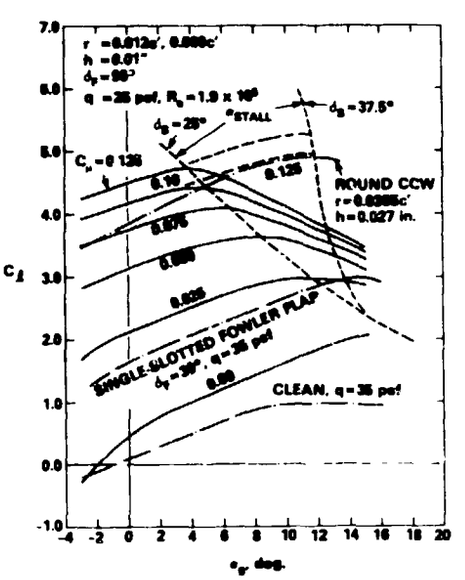

Fig. 20 - Lift Variation with Incidence for Dual Radius CCW Configuration B, $c_f = 0.035c'$

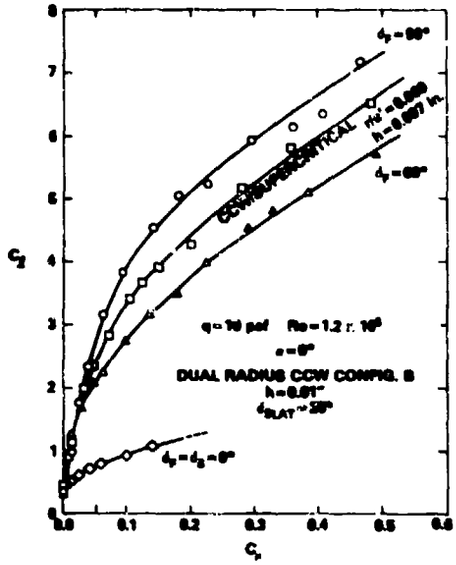

Fig. 21 - Lift at Higher Blowing Rates

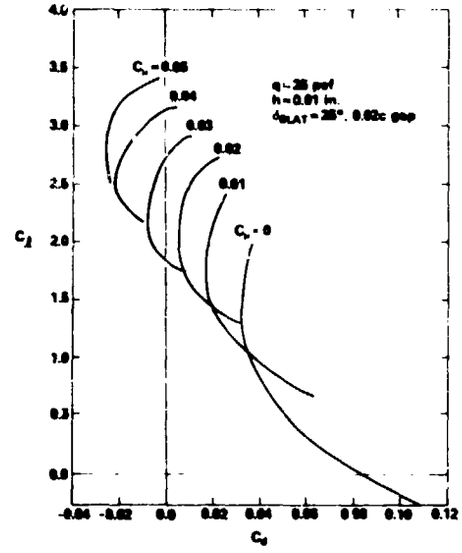

Fig. 22 - Drag Polars at Constant Blowing for Dual Radius CCW Configuration A, $c_f = 0.0223c'$

The effect of extending the available blowing range was investigated by reducing the dynamic pressure to 10 psf so that available pressure and mass flow would yield higher C_μ. Figure 21 shows the high lift obtained by the larger-chord dual radius CCW in comparison to the CCW/Supercritical airfoil. Because the secondary radius exceeds that of the supercritical airfoil, so also does the lift. The generation of C_ℓ approaching 8 at 0 degrees incidence appears quite promising, should the increased C_μ be available. In these higher blowing ranges, lift is nearly a linear function of C_μ for either blown flap or full-round CCW trailing edge.

Drag and Pitching Moment with Blowing

Drag polars at constant C_μ are shown in Figure 22 for the shorter-flap dual radius CCW configuration A, but the trends are similar for the other CCW geometries. In general, for a constant α_g, increase in C_μ results in reduced drag as thrust is recovered from the jet itself. In this figure, the initial high drag levels at low C_μ and incidence are due to the 90-degree flap and separated flow on the slat lower surface (at no blowing and $\alpha_g = 0$ degrees, it's operating at -25 degrees local incidence.) These data are of course 2-D values and do not address the 3-D induced drag component due to lift, which will become the dominant drag value for finite wing configurations.

Figure 23 depicts quarter-chord pitching moment variation with lift as a function of blowing incidence for the larger dual radius configuration B. Lift generated by increasing blowing at constant incidence yields greater nose-down moment due to the trailing edge suction peaks. Conversely, lift generated by increasing α_g beyond 3 degrees at constant C_μ yields lesser nose-down moment due to leading edge suction peaks. A comparison with the other CCW data shows very similar trends, but indicates that for the same α_g and C_ℓ, the smaller radius will yield more nose-down pitch, again due to greater trailing edge suction peaks. Similar nose-down pitch levels were trimmable with modification to the existing stabilizer on the A-6/CCW flight demonstrator.

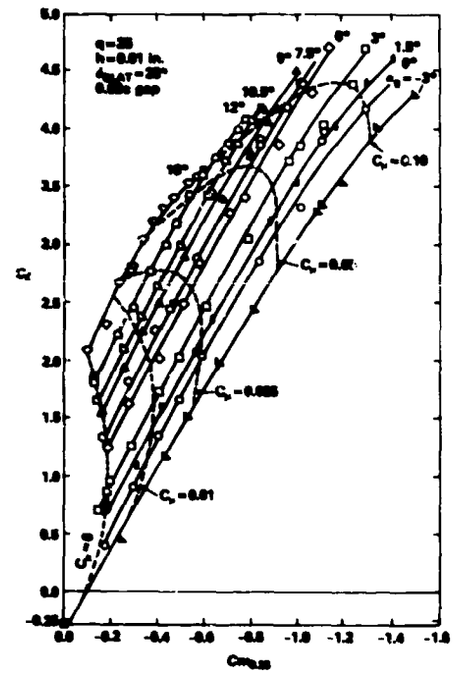

Fig. 23 - Pitching Moment of the Dual Radius CCW Configuration B, $c_f = 0.035c'$

Blowing-off Comparison

A major design goal of an improved high lift airfoil was to minimize any cruise drag penalty. The various A-6 blown airfoils tested above are compared in their clean configurations in Figure 24, where slat, flap and circular arc trailing edge were retracted; small and mini CCW trailing edges were left deployed, but the slat was retracted. The clean blown flap is considered to be the same configuration as the clean cruise airfoil. As the CCW trailing edge thickness increased, so also

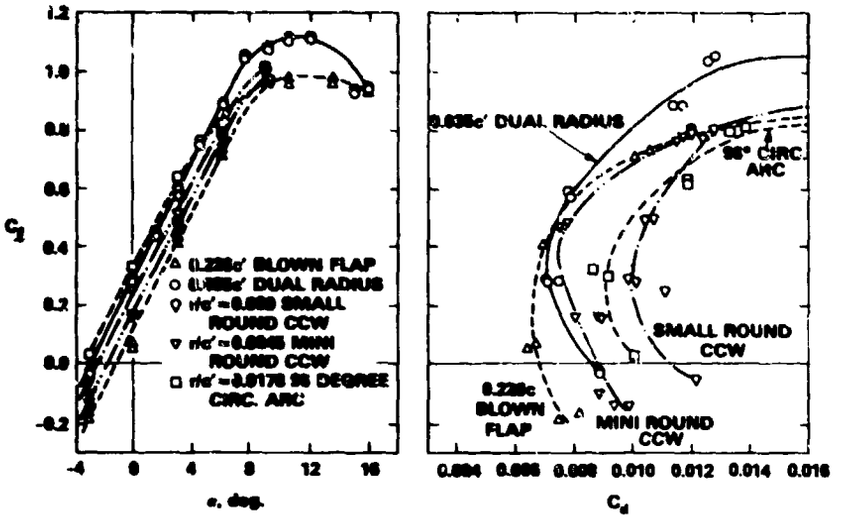

Fig. 24 - Blowing-off Clean Airfoil Comparison

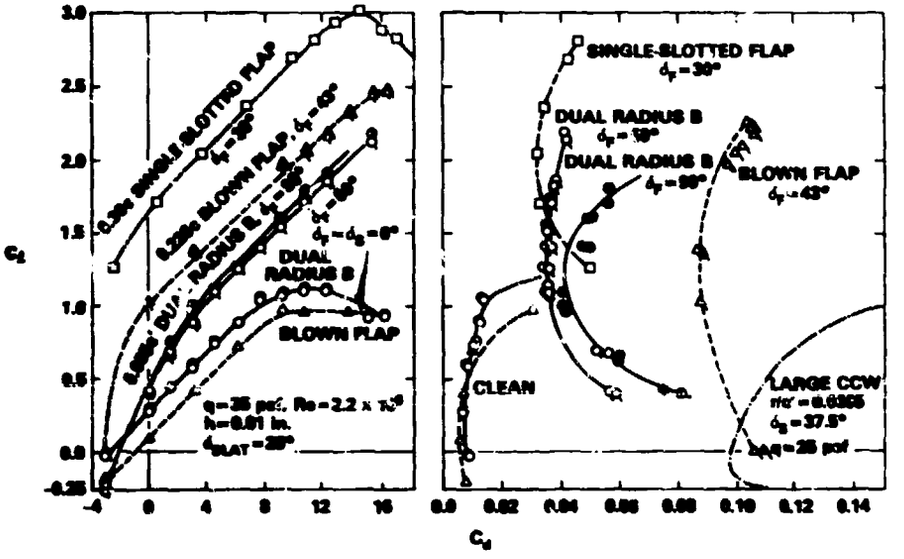

Fig. 25 - Effect of Blowing-off Flap Deflection

did the aft camber and resulting lift due to camber; the 96-degree circular arc shifted the lift curve upwards by an increment of 0.21 over the clean airfoil. Along with this thickness, camber and lift increases cause a corresponding drag increase, as shown by the drag polars. The one exception was the dual radius configuration, whose large secondary radius ended in a thin near-sharp trailing edge, thus avoiding aft surface flow separation. In fact, for $C_\ell > 0.5$, the dual radius yielded less drag than the clean airfoil, probably because the clean airfoil required higher angle of attack to reach the same C_ℓ.

The effect of deflecting the flap on the various configurations without blowing is shown in Figure 25; this comparison may be relevant to predicting takeoff, waveoff, and approach conditions should a total blowing failure occur. Increasing aft camber by increasing either flap chord length or deflection shows significant lift increases. It also shows significant profile drag increase, with the exception of the baseline single-slotted flap, where separation drag is probably avoided by the flow through the slot. The unslotted blown flap yields the highest drag levels of the above configurations. As a final comparison, the unacceptable unblown drag of the original large chord CCW of Figure 1 is shown. All airfoils tested improved on this configuration. The minimum drag of the 90-degree flap dual radius CCW is about 40% that of the larger radius and occurs at much higher C_ℓ. At the same C_ℓ (say 1.0), the unblown dual radius drag is 25 percent of the large radius, and less at higher C_ℓ. In general, the drag levels of these small trailing edges show considerable improvement over those of the original larger trailing edge radius.

Conclusions and Recommendations

A series of reduced-size CCW trailing edge configurations has been developed and subsonically evaluated in a program to reduce the complexity, size and weight of the CCW high lift system, while maintaining the high lift previously generated and reducing or eliminating the unblown cruise drag penalty of the thick trailing edge. The following conclusions resulted from these investigations:

- A small round trailing edge could be incorporated into the existing aft contour of a thick supercritical airfoil. On this airfoil, a radius 1/4 the size of the original A-6/CCW airfoil ($r/c' = 0.0365$) yielded slightly greater lift, producing lift coefficients near 7 at $\alpha = 0$ degrees and $C_\mu < 0.5$. Furthermore the large undeflected leading edge radius of the supercritical airfoil provided the same leading edge stall prevention as did the 37.5-degree slat of the A-6/CCW.

- Base drag was sufficiently reduced by the small trailing edge radius, so that unblown subsonic C_d was nearly the same as the baseline supercritical airfoil, or could be reduced to less than the baseline by a minimal amount of blowing.

- Of the single-radius CCW configurations applied to the thin A-6 airfoil section, the largest radii produced the greatest lift, as long as there was sufficient arc length to maintain jet turning (150 degrees was sufficient, 96 degrees provided less lift). Too small a radius produced lift reductions after a certain blowing pressure ratio was reached.

- The dual radius CCW provided an effective means to maintain a large radius, sufficient jet turning and a thin trailing edge for cruise. A 0.035c' flap dual radius configuration produced greater lift than the original thick radius A-6/CCW; at $\alpha_R = 0$ degrees, C_ℓ greater than 7 was generated by $C_\mu < 0.5$. For a more practical C_μ value of 0.125 and 9 degrees incidence, C_ℓ of 5.2 could be generated compared to the baseline single-slotted mechanical flap C_ℓ of 2.6 at the same incidence.

- Blowing-off drag for the 90-degree short chord dual radius airfoil was greatly reduced over both the original large CCW and a 0.226c blown flap. In the clean configuration with no flap deflection, subsonic drag was nearly the same or slightly less than the A-6 cruise airfoil. Lift due to trailing edge camber could allow cruise at lower angle of attack, thus resulting in the reduced drag level. All trailing edges investigated produced less 2-D drag than the original larger radius A-6/CCW configuration.

These results suggest the strong potential of two advanced forms of the Circulation Control Wing airfoil:

- A CCW/Supercritical no-moving-parts configuration with no need for a deflecting leading edge device, and transition from the cruise to high lift modes by initiation of blowing.

- A thinner high performance CCW airfoil with a small-chord dual radius flap and some type (blown or mechanical) of effective leading edge device. The flap geometry would provide no cruise penalty (actually the availability of a blowing slot for maneuverability or cruise drag reduction could be quite beneficial), and its larger secondary radius would provide even greater lift than large single-radius configurations. The strength of the dual radius airfoil lies in its ability to provide a large turning radius, arc length and jet turning angle accompanied by a very simple conversion to a near-conventional cruise airfoil.

The above data confirm the subsonic feasibility of two families of improved CCW airfoils to generate excellent STOL performance with little or no cruise penalty and without the weight, complexity and size of conventional mechanical or powered high lift systems. The remaining unknown is the effect of the trailing edge geometries on the airfoil characteristics in high subsonic or transonic flow. This concern will be addressed in transonic 2-D wind tunnel investigations which are now planned in order to complete the DTNSRDC program for development of these advanced airfoils.

References

1. Englar, R.J., et al., "Circulation Control — An Updated Bibliography of DTNSRDC Research and Selected Outside References," DTNSRDC Report 77-0076 (Sept 1977).

2. Englar, R.J., et al., "Design of the Circulation Control Wing STOL Demonstrator Aircraft," AIAA Paper No. 79-1842 presented at the AIAA Aircraft Systems and Technology Meeting, New York (Aug 1979). Republished in AIAA Journal of Aircraft, Vol. 18, No. 1, pp 51-58 (Jan 1981).

3. Pugliese, A.J. and R.J. Englar, "Flight Testing the Circulation Control Wing," AIAA Paper No. 79-1791 presented at AIAA Aircraft Systems and Technology Meeting, New York (Aug 1979).

4. Englar, R.J., "Development of the A-6/Circulation Control Wing Flight Demonstrator Configuration," DTNSRDC Report ASED-79/01 (Jan 1979).

5. Englar, R.J., "Subsonic Two-Dimensional Wind Tunnel Investigations of the High Lift Capability of Circulation Control Wing Sections," DTNSRDC Report ASED-274 (Apr 1975).

6. Nichols, J.H., Jr., et al., "Experimental Development of an Advanced Circulation Control Wing System for Navy STOL Aircraft," AIAA Paper No. 81-0151 presented at the AIAA 19th Aerospace Sciences Meeting, St. Louis (12-15 Jan 1981).

7. McGhee, R.H. and G.H. Bingham, "Low-Speed Aerodynamic Characteristics of a 17-percent Thick Supercritical Airfoil Section, Including a Comparison Between Wind-Tunnel and Flight Data," NASA TM X-2571 (Jul 1972).

8. Englar, R.J., "Low-Speed Aerodynamic Characteristics of a Small, Fixed-Trailing Edge Circulation Control Wing Configuration Fitted to a Supercritical Airfoil," DTNSRDC Report ASED-81/08 (Mar 1981).

9. Englar, R.J., "Development of an Advanced No-Moving Parts High-Lift Airfoil" Paper ICAS-82-6.5.4 in Proceedings of ICAS/AIAA Aircraft System and Technology Conference, Seattle (22-27 Aug 1982).

10. Grumman Aerospace Corporation Report No. WS-128 ( )-R-4, Vol. I, "Wind Tunnel Test Report — 2D NSRDC Test of a 64A008.4 Mod Airfoil, Blown Flaps Phase." (Feb 1983).

11. Englar, R.J. and J. Ottensoser, "Calibration of Some Subsonic Wind Tunnel Inserts for Two-Dimensional Airfoil Experiments," DTNSRDC Report ASED AL-275 (Sep 1972).

12. Englar, R.J., "Two-Dimensional Subsonic Wind Tunnel Test of a Cambered 30-Percent Thick Circulation Control Airfoil," DTNSRDC Report ASED AL-201 (May 1972).

INITIAL DISTRIBUTION

Copies		Copies	
1	DARPA (AVTO)/LCOL Allburn		NAVAIR (continued)
1	ASN (RE&S)/Asst for Aircraft		1 AIR-05
1	OSD (DDR&E)/R. Siewert		1 AIR-528
5	CNO		1 AIR-5301
	1 OPNAV-05/VADM Schoultz		1 AIR-5360C4/R. Groeselfinger
	1 OPNAV-05V/CAPT Cargill	1	NISC/LT Huska
	1 OPNAV-506C	2	NWC
	1 OPNAV-50W1/R. Thompson		1 Tech Library
	1 OPNAV-50W1/CAPT Seibert		1 Code 3304/P. Amundsen
1	CMC/Science Advisor	3	NAVAIRTESTCEN
3	ONR		1 DIR TPS
	1 Code 210/CAPT Howard		1 SA-04C/M. Branch
	1 Code 432/R. Whitehead		1 J. Hoeg
	1 Code 100M/COL R. Bowles	1	NAVPRO/Bethpage/L. Meckler
1	NRL/Tech Library	12	DTIC
3	NAVMAT	1	DIA/P. Scheurich
	1 07P/J. Enig		
	1 071/O. Remson	7	AFWAL
	1 08D4/H. Moore		1 FIX/M. Silverman
1	NAVPGSCOL/ Tech Library		1 FDV/STOL Tech Div
			1 FDMM/Aeromech Br
6	NAVAIRDEVCEN		1 FIMM/D. Bowers
	1 Tech Dir		1 FS/K. Richey
	1 Tech Library		1 AFIT/M. Franke
	1 K. Green		1 ASD/XRS/F. Krause
	1 C. Mazza	1	AFOSR/Aero Sciences
	1 T. Miller		
	1 B. Antinelli	1	FAA/Code DS-22, V/STOL
14	NAVAIRSYSCOM	2	NASA HQ
	1 AIR-00D4/Tech Library		1 R. Winblade
	1 AIR-03		1 R. Wasicko
	1 AIR-03A/E. Cooper		
	1 AIR-03B/H. Andrews		
	1 AIR-303	5	NASA Ames Res Cen
	1 AIR-310/T. Momiyama		1 Tech Library
	1 AIR-310C/D. Hutchins		1 Full-Scale Aero Br
	1 AIR-310D/J. Nichols		1 Large-Scale Aero Br
	1 PMA-234		1 FVQ/D. Riddle
	1 PMA-244		1 A. Faye

Copies	
2	NASA Dryden 1 Tech Library 1 T. Ayers
7	NASA Langley Res Cen 1 Tech Library 1 TEPO/J. Pyle 1 R. Margusou 1 J. Campbell 1 H. Garner 1 R. Barnwell 1 Code 286/J. Paulsen
1	California Inst Tech/ Dept of Aeronautics
1	Cornell University/Tech Lib
1	U of Kansas/Aero Engr Lib
1	U of Maryland/A. Gessow
1	U of West Va/Aero Engr Lib
1	Analytical Methods, Inc F. Dvorak
1	Beech Aircraft Corp/Tech Lib
2	Boeing Comm Airplane Co/Seattle 1 Tech Library 1 W. Clay
2	Boeing Mil Airplane Co/Wichita 1 Tech Library 1 L. Frutiger
3	Douglas Aircraft Co 1 Tech Library 1 P. McGowan 1 F. Posch
1	Flight Craft Inc/R. Griswold
1	Franklin Research Center C. Belsterling
2	General Electric Co 1 Tech Library 1 T. Stirgwolt

Copies	
3	General Dynamics/Ft. Worth 1 Tech Library 1 W. Foley 1 W. Woodrey
1	General Dynamics/San Diego Tech Library
4	Grumman Aerospace Corp 1 Tech Library 1 M. Ciminera 1 E. Miller 1 M. Siegel
1	Honeywell, Inc/S&R Div
2	Hughes Helicopters 1 Tech Library 1 A. Logan
2	Kaman Aerospace Corp 1 Tech Library 1 D. Barnes
1	Kohlman Aviation Corp
5	Ling-Temco-Vought, Inc 1 Tech Library 1 K. Krall 1 J. Louthan 1 H. Scherrieb 1 S. Wells
3	Lockheed California Co 1 Tech Library 1 A. Yackel 1 H. Yang
3	Lockheed Georgia Co 1 Tech Library 1 C. Dixon 1 J. Viney
2	Northrop Corp/Aircraft Div 1 Tech Library 1 W. A. Lusby
1	Pratt & Whitney Aircraft/ Gov't Products Div L. Oglesby

Copies

Copies		
3	Rockwell International/Columbus	
	1	Tech Library
	1	P. Bevilaqua
	1	W. Palmer
2	Rockwell International/LA	
	1	Tech Library
	1	M. Robinson
2	Teledyne Ryan Aeronautical	
	1	Tech Library
	1	W. Ebner
1	United Technologies Corp/ E. Hartford/Tech Lib	

CENTER DISTRIBUTION

Copies	Code	Name
1	012.3	Research Coordinator
2	1606	Aerodynamics Collection
1	1606	C. Applegate
10	1660	R. Englar
10	5211.1	Reports Distribution
1	522.1	Library (C)
1	522.2	Library (A)
1	9300	Patent Counsel

DTNSRDC ISSUES THREE TYPES OF REPORTS

1. DTNSRDC REPORTS, A FORMAL SERIES, CONTAIN INFORMATION OF PERMANENT TECHNICAL VALUE. THEY CARRY A CONSECUTIVE NUMERICAL IDENTIFICATION REGARDLESS OF THEIR CLASSIFICATION OR THE ORIGINATING DEPARTMENT.

2. DEPARTMENTAL REPORTS, A SEMIFORMAL SERIES, CONTAIN INFORMATION OF A PRELIMINARY, TEMPORARY, OR PROPRIETARY NATURE OR OF LIMITED INTEREST OR SIGNIFICANCE. THEY CARRY A DEPARTMENTAL ALPHANUMERICAL IDENTIFICATION.

3. TECHNICAL MEMORANDA, AN INFORMAL SERIES, CONTAIN TECHNICAL DOCUMENTATION OF LIMITED USE AND INTEREST. THEY ARE PRIMARILY WORKING PAPERS INTENDED FOR INTERNAL USE. THEY CARRY AN IDENTIFYING NUMBER WHICH INDICATES THEIR TYPE AND THE NUMERICAL CODE OF THE ORIGINATING DEPARTMENT. ANY DISTRIBUTION OUTSIDE DTNSRDC MUST BE APPROVED BY THE HEAD OF THE ORIGINATING DEPARTMENT ON A CASE-BY-CASE BASIS.